Applied Surface Science 466 (2019) 801–807

Contents lists available at ScienceDirect

Applied Surface Science

journal homepage: www.elsevier.com/locate/apsusc

Full Length Article

Modified strain and elastic energy behavior of Ge islands formed on high-miscut Si(0 0 1) substrates

L.A.B. Marçal[a,b], M.-I. Richard[a,c], L. Persichetti[d], V. Favre-Nicolin[a], H. Renevier[e,f], M. Fanfoni[g], A. Sgarlata[g], T.Ü. Schülli[a], A. Malachias[b,*]

[a] European Synchrotron Radiation Facility, CS 40220, 38043 Grenoble Cedex 9, France
[b] Departamento de Física, ICEx, Universidade Federal de Minas Gerais – UFMG, Av. Antonio Carlos, 6627 Belo Horizonte – MG, CEP 30123-970, Brazil
[c] Aix-Marseille University, IM2NP-CNRS, Faculté des Sciences de St Jérôme, 13397 Marseille, France
[d] Dipartimento di Scienze, Università Roma Tre, Viale G. Marconi, 446- 00146 Rome, Italy
[e] Univ. Grenoble Alpes, LMGP, F-38000 Grenoble, France
[f] CNRS, LMGP, F-38000 Grenoble, France
[g] Dipartimento di Fisica, Universitàdi Roma "TorVergata", Via della Ricerca Scientifica, 1-00133 Roma, Italy

ARTICLE INFO

Keywords:
Ge islands
Miscut
Faceting
Synchrotron x-ray diffraction
Finite elements simulations

ABSTRACT

We investigate here the influence of Si substrate miscut on the strain and elastic energy of Ge islands. We show how the morphology, composition and the elastic energy for 4 and 13 monolayers (ML) Ge islands grown at 600 °C and 730 °C on vicinal Si(0 0 1) surfaces change with miscut angles ranging between 0° and 10°. Scanning Tunneling Microscopy is used to determine the island morphology. Resonant x-ray diffraction near the Ge-K absorption edge allows the determination of the Ge concentration as well as the elastic energy stored on such structures from their dependency on the lattice parameter. Simulations using the Finite Elements Method indicate that the enlargement of the SiGe broad peak retrieved from the x-ray diffraction measurements is actually caused by the asymmetrical faceting induced by large miscut angles. Such faceting has a strong effect on island density and elastic energy, producing differences that are proportional to those observed in conditions with distinct SiGe content.

1. Introduction

Self-assembled semiconductor nanostructures have been intensively investigated in the past decades. In particular, the interest in obtaining either spatially ordered islands [1,2] and/or with the enhancement of specific crystal facets [3–6] has driven recent interest to the use of substrates with distinct surface conditions [1,7]. It is known that both high crystallographic index oriented substrates as well as the surfaces with crystal steps introduced by a miscut angle affect the growing process at the nanoscale [8,9] and alter the symmetry of the elastic-interaction potential between epitaxial nanostructures [10]. The ability to control optoelectronic properties due to elastic tensor constraints in these structures plays an important role for modern nanoscale engineering [11–14]. Finally, surface configurations and energies of the vastly studied heteroepitaxial growth of Ge islands on vicinal Si(0 0 1) can be also better understood when compared to similar objects grown on substrates with miscut [4,15–17].

On Si(0 0 1) substrates, the coverage-dependent evolution of islands shape and size is well understood. There are characteristic transitions from unfaceted prepyramids to {1 0 5} faceted SiGe pyramidal huts up to multifaceted domes and superdomes increasing the Ge concentration [18–20]. In this work we study Si/Ge intermixing, as well as the elastic energy stored in the nanostructures, for a set of samples with different nominal Ge coverages (4 ML and 13 ML), located within the vicinal pyramidal and dome/superdome regimes, grown at distinct temperatures (600 °C and 730 °C). The retrieved information on strain fields, elastic energy and composition (using resonant synchrotron x-ray diffraction) is compared for islands grown on substrates with and without miscut.

2. Experimental section

2.1. Sample preparation

The samples studied in this work consist of SiGe islands grown on Si (0 0 1)substrates. The islands were grown by physical-vapor deposition

* Corresponding author.
E-mail address: angeloms@fisica.ufmg.br (A. Malachias).

https://doi.org/10.1016/j.apsusc.2018.10.094
Received 12 July 2018; Accepted 11 October 2018
Available online 12 October 2018
0169-4332/

of Ge on the singular Si(0 0 1) surface and on vicinal substrates misoriented by 6° and 10° towards the [1 1 0] direction at T = 600 °C and 730 °C and at constant flux of 1.8×10^{-3} ML/s. In order to verify the island morphology, scanning tunneling microscopy (STM) measurements were carried out *in situ* by using a scanning tunneling microscope under ultra high-vacuum conditions ($p < 3 \times 10^{-11}$ torr) [21].

2.2. Characterization

Synchrotron grazing-incidence x-ray diffraction measurements were carried out at the ID01 and BM02 beamlines of the European Synchrotron Radiation Facility (ESRF, Grenoble), as well as at the XRD2 beamline of the Brazilian Synchrotron Light Laboratory (LNLS, Campinas). The experiments were performed using 6-circle (BM02 and XRD2) and 3 + 2-circles (ID01) diffractometers equipped with area detectors (Maxipix, Pilatus 100 K). The incident angle was fixed at the critical angle of total external reflection (0.16°) near 11.103 keV (K-absorption edge of Ge). The diffracted signal was measured over a minimum exit angle range of 1.5°.

Finite Elements Method (FEM) analysis using a commercial software package (COMSOL Multiphysics) was carried out to simulate the displacement and strain fields inside the measured islands, and then to simulate their scattering signal.

3. Results and discussion

3.1. Morphology characterization

Fig. 1(a) and (b) display the STM images obtained for the samples with 4 ML of Ge coverage grown at 600 °C on a Si(0 0 1) substrate without miscut and with 10° miscut, respectively. On the flat substrate (0° miscut), a mixture of {1 0 5} faceted pyramids and domes is

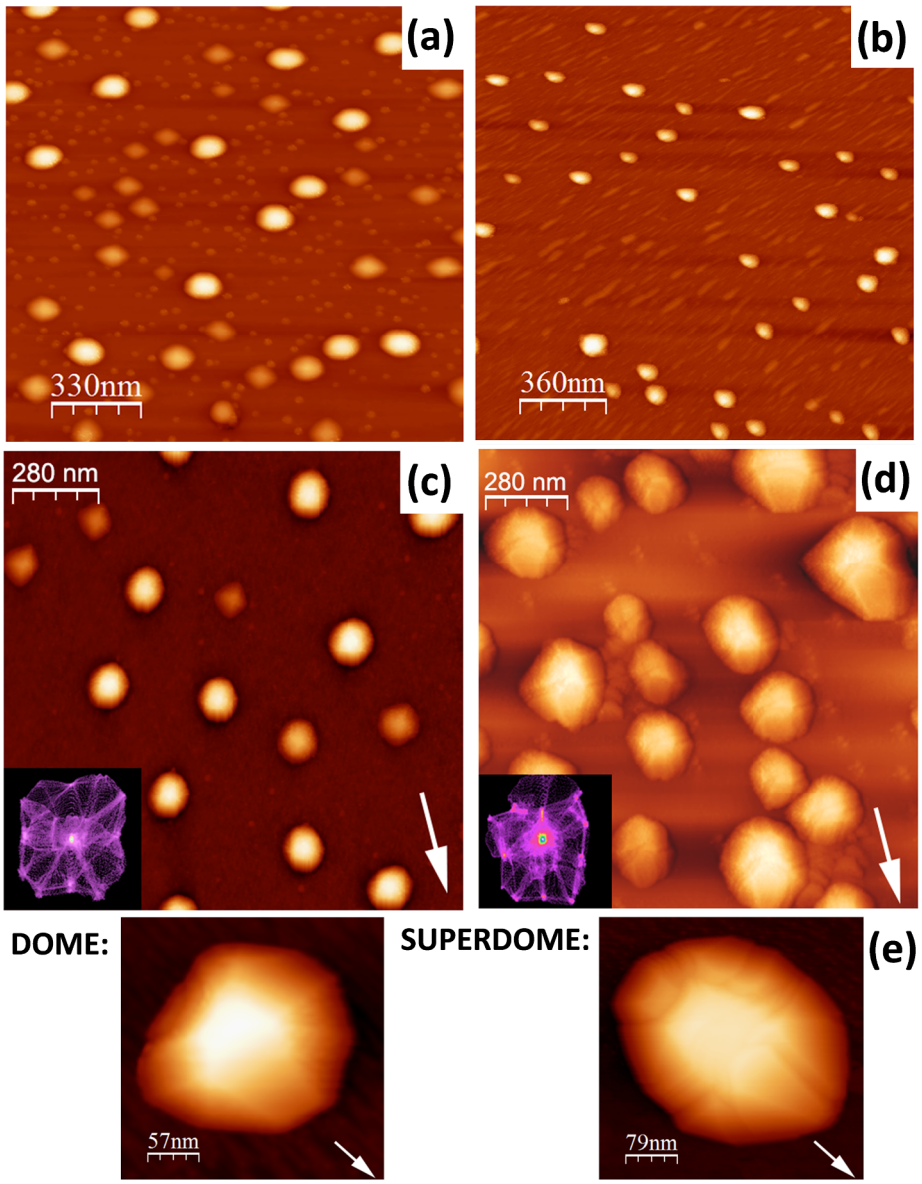

Fig. 1. Scanning Tunneling Microscopy images showing the morphology of islands on the (a) 4 ML sample without miscut, (b) 4 ML sample with 10° miscut, (c) 13 ML sample without miscut and (d) 13 ML sample with 10° miscut. All of the images correspond to samples grown at 600 °C. The insets show the facets of the structures. It is possible to notice a longer semi-axis along the [1 1 0] direction (indicated by arrows in the STM images for the 13 ML samples) for the sample with miscut. Figure (e) shows a zoom for a dome and a superdome from the 13 ML sample, evidencing the stretching on the superdome at the [1 1 0] direction.

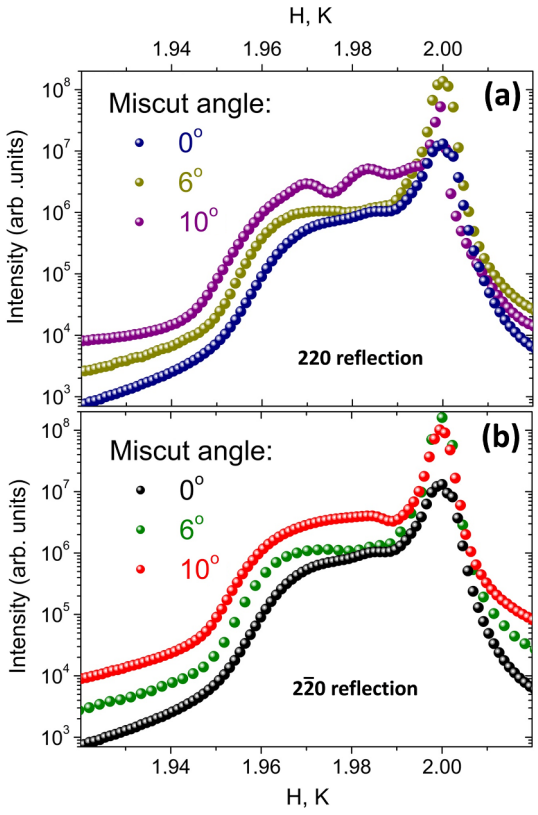

Fig. 2. Longitudinal x-ray diffraction scans near the (a) (2 2 0) and (b) (2 $\bar{2}$ 0) reflections for the sample with 13 ML Ge (T_G = 600 °C). The presence of features between H, K = 1.97 and H, K = 1.99 indicates distinct faceting from each direction.

observed, while for the 10° miscut sample, the growth of the pyramids is hindered by the geometrical constraint of the miscut angle, and instead a wetting layer completely faceted by {1 0 5} ripples appears, so the domes and a {1 0 5} faceted wetting layer can be found. For the sample with 4 ML coverage and without miscut. the two observed types of islands have different densities: pyramids correspond to 85% of the islands and domes to 15%, resulting in an overall density of 12×10^9 islands/cm^2. The average height and lateral size of the domes are (23 ± 6) nm and (110 ± 20) nm, respectively. Conversely, the pyramids are (5 ± 2) nm in height and (50 ± 10) nm in lateral dimension. Only domes are observed on the 10° miscut sample, with a density of 1.8×10^9 islands/cm^2, and average height of (15 ± 2) nm and a lateral size of (80 ± 20) nm. Fig. 1(c) and (d) show STM images obtained for the samples with 13 ML of Ge on 0° and 10° miscut substrates, respectively. One notices that the average length of one of the semiaxis along the [1 1 0] direction increases for larger miscut angles. On the other hand, island density is reduced, which indicates that the material deposited is re-distributed among islands. From the images, one can see that the sample with 0° miscut and 13 ML coverage contains nanostructures with an average height of (15 ± 2) nm and a length of (110 ± 20) nm along the longer semiaxis. Instend for the islands on the 10° miscut substrate, a height of (23 ± 6) nm and a length of (190 ± 40) nm (longer semiaxis) are observed. At 13 ML of Ge coverage, 15% of the island population consists of superdomes. The islands density is about 1.7×10^9 islands/cm^2 for the flat substrate and 0.9×10^9 islands/cm^2 for the substrate with 10° miscut. Fig. 1(e) displays one isolated dome and one superdome, from the 13 ML sample, evidencing the differences on sizes, specially along the [1 1 0] direction.

3.2. X-ray diffraction analysis

To seek distinct lattice relaxation responses caused by any strain anisotropy that may take place due to islands shape, surface x-ray measurements along perpendicular directions were performed for the sample with 13 ML of Ge coverage grown at 600 °C. Fig. 2(a) and (b) show x-ray diffraction longitudinal (radial) profiles along the [2 2 0] and [2 $\bar{2}$ 0] directions, respectively. One narrow and intense peak coming from the Si substrate is observed at H = K = 2 (reciprocal lattice units of Si) for each of the two scans. A broad peak extends towards lower values of (H, K), corresponding to larger local lattice parameters. It is attributed to the presence of a gradient of lattice parameter values inside the Ge nanostructures [22]. The intensity signal drop around H, K = 1.945 for both reflections indicates that asymmetries on the strain distribution are not significant comparing both in-plane directions. Nevertheless, the distinct faceting from each direction generates features between H, K = 1.97 and H, K = 1.99.

Fig. 3 shows longitudinal scans measured near the **220** Si Bragg peak for the samples containing 4 ML (a) and 13 ML (b) of Ge coverage, grown on Si substrates with 0° and 10° of miscut. The broad intensity distribution observed for the scans corresponding to the samples with 10° miscut reach lower (H, K) values compared to the signal of islands grown on the flat substrate for both 4 and 13 ML. Higher diffracted intensities were also detected at lower (H, K) values, indicating the existence of more material with partially or fully relaxed lattice parameter in these structures. These results suggest that for larger miscut angles, the Ge concentration increases inside islands.

The Ge composition in all samples was retrieved performing resonant (anomalous) x-ray diffraction measurements. Fig. 4 shows longitudinal scans for three different photon energies: (i) 80 eV below the Ge K absorption edge, (ii) 6 eV below the edge, and (iii) on resonance with the edge. Panel (a) is referred to the sample grown at 600 °C with no miscut, (b) to the sample grown at 730 °C with no miscut and (c) to the sample grown at 600 °C with 10° miscut for Ge coverage of 4 ML. For all the three samples, it is clear that the diffracted intensity from the domes decreases as the energy gets closer to the edge. This effect is stronger for the samples grown at 600 °C, which is consistent with a reduced Si interdiffusion at lower growth temperature, leading, in turns, to domes with larger Ge content. This result is in agreement with the data measured on samples grown at 730 °C reported in Fig. 4(b), where narrower peak for the domes indicates a lower Ge concentration, since the observed lattice parameter distribution does not span significantly towards the value of bulk Ge. Differences between the samples grown at 600 °C with and without miscut cannot be directly noticed at this point.

The dependency of the intensity of the diffracted beam with the Ge concentration is quantified using Eq. (1) [22,23]:

$$I^{SiGe} = I_0 |C_{Ge} f_{Ge} + C_{Si} f_{Si}|^2$$

$$= I_0 |C_{Ge} (f_{Ge} - f_{Si}) + f_{Si}|^2 \quad (1)$$

where I^{SiGe} is the intensity for a given energy, I_0 is a normalization constant that depends on the beam flux, C_{Ge}, C_{Si}, f_{Ge} and f_{Si} are the concentrations and the atomic scattering factors for the Ge and Si, respectively.

Applying Eq. (1) on the resonant x-ray scattering data, we obtain the Ge concentration, since f_{Ge} and f_{Si} are known for a given energy and I^{SiGe} can be retrieved from the measurements, leaving only I_0 and C_{Ge} unknown. Varying the normalization constant and the Ge concentration, with fixed values of scattering factors for each energy, we found the optimal fitting for the variables that matches each calculated I^{SiGe} to the corresponding measured intensities. Minimizing the differences from the theoretical and experimental outputs for the three energies,

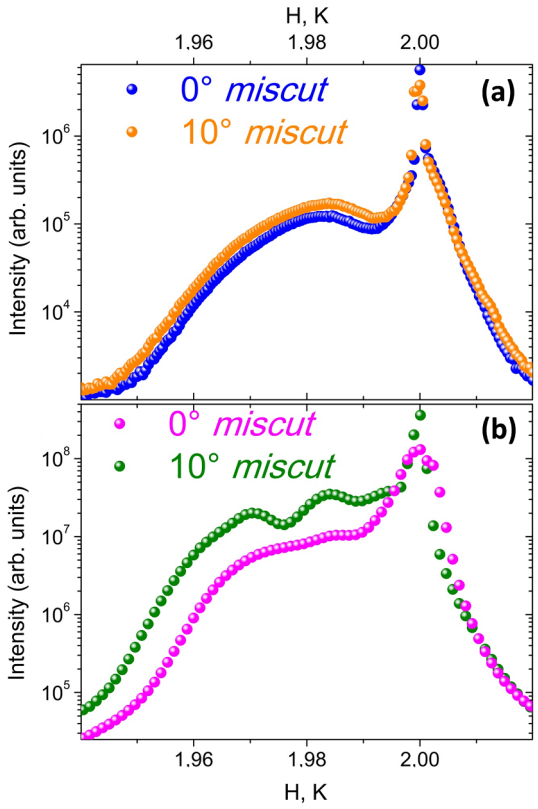

Fig. 3. Longitudinal x-ray diffraction scans are shown for the samples containing (a) 4 ML and (b) 13 ML of Ge coverage grown at 0° and 10° miscut under 600 °C. The diffraction peaks corresponding to the islands span a larger range of (H, K) values for the samples with miscut angle, suggesting a larger Ge concentration in the domes and superdomes grown on substrates with miscut.

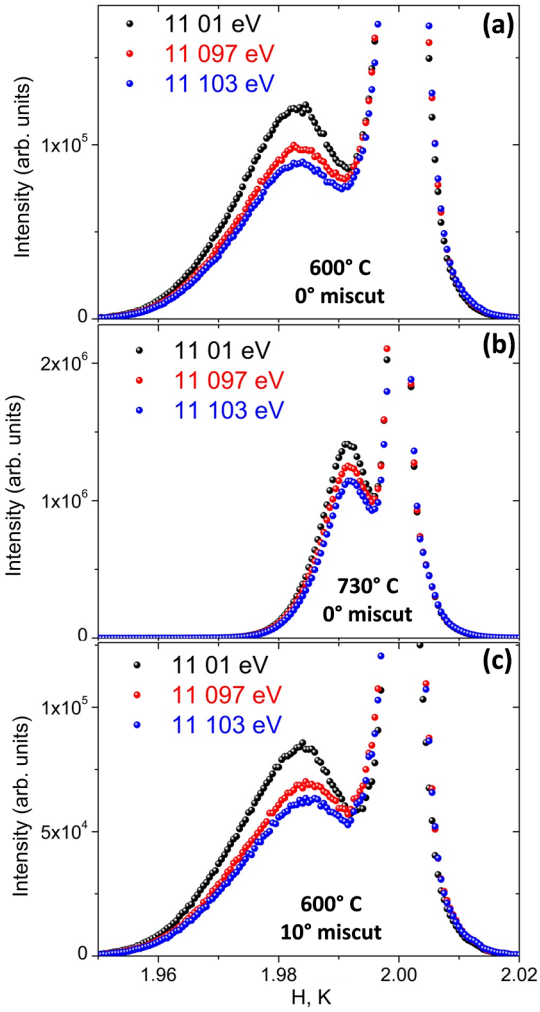

Fig. 4. Resonant x-ray diffraction longitudinal scans performed near the Si **220** Bragg peak for (a) the sample grown at 600 °C with no miscut, (b) the sample grown at 730 °C with no miscut and (c) the sample grown at 600 °C with 10° miscut. All results in this figure refer to 4 ML samples. The photon energies used were: 93 eV below the Ge K absorption edge (black dots), 6 eV below the edge (red dots), and at the Ge-K edge (blue dots).

simultaneously, C_{Ge} becomes unambiguously determined. The procedure was used for different values of (H, K), allowing us to plot the Ge concentration as a function of the in-plane lattice parameter condition, for each of the studied samples. The left panels from Fig. 5 show the Ge concentration results for the samples grown at (a) 600 °C (4 ML Ge), (b) 730 °C (4 ML Ge) and (c) at 600 °C (13 ML Ge), with 0° and 10° miscut for the first two sets of samples and 0° and 6° miscut for the last one. Clearly, the Ge concentration is reduced in the direction where the in-plane lattice parameter moves towards the bulk Si value. For larger lattice parameter values, the local Ge content increases in all cases. One notices that for the 4 ML (600 °C) samples, the Ge concentration is larger for islands grown on substrates with miscut, if compared with the flat surfaces. Such result indicates that the island facets, which become larger after growth on substrates with miscut, may present a larger barrier against surface diffusion of Si atoms. This scenario changes when we look at the samples with a deposit of 13 ML of Ge (600 °C), where a larger Ge content is retrieved at the flat substrate condition. Such effect indicates that the {1 1 1} facets at the base of superdomes (which are present at this coverage) become larger for the substrates with miscut, and are preferential sites for Si diffusion from the substrate [24].

The right panels of Fig. 5 show the elastic energy per atom, displayed as a function of the local lattice parameter for each sample. From Fig. 5(d), it can be noticed that the elastic energy is higher when the miscut substrate is used for the samples grown at 600 °C with 4 ML of Ge coverage. The same scenario holds for the samples grown at 730 °C (4 ML Ge) and at 600 °C (13 ML Ge), as shown in Fig. 5(e) and (f) respectively, up to large lattice parameters, corresponding to the domes/superdomes regime. The elastic energy assumes values close to 0 when the lattice parameter approaches that of the bulk Si, while it increases for the region corresponding to the islands. This result indicates that the symmetry break introduced by the large island facets on substrates with miscut drives the system away from the usual minimum energy condition [21,25].

3.3. Finite Elements Method simulation

Finite Elements Method analysis using a commercial software package (COMSOL Multiphysics) was performed to simulate islands with 4 ML Ge coverage grown at 600 °C. These simulations were carried out to understand whether the broadening of the diffraction peak coming from the Ge islands grown on substrates with and without miscut is due to surface or bulk effects. Fig. 6(a) shows cross-section images for the two simulated structures, the upper one without miscut and the bottom one with 10° miscut. The colormap shows the displacement $\boldsymbol{u}$ after relaxation, evidencing the asymmetry of strain distribution on the samples with miscut. A visual comparison of equal-volume islands, such as those depicted in Fig. 6(a), is not enough to identify in which island the largest amount of elastic energy is stored. Due to the effect of the asymmetric morphology on the island, variables must be evaluated for the whole volume.

The geometrical asymmetry has, nevertheless, a clear signature on

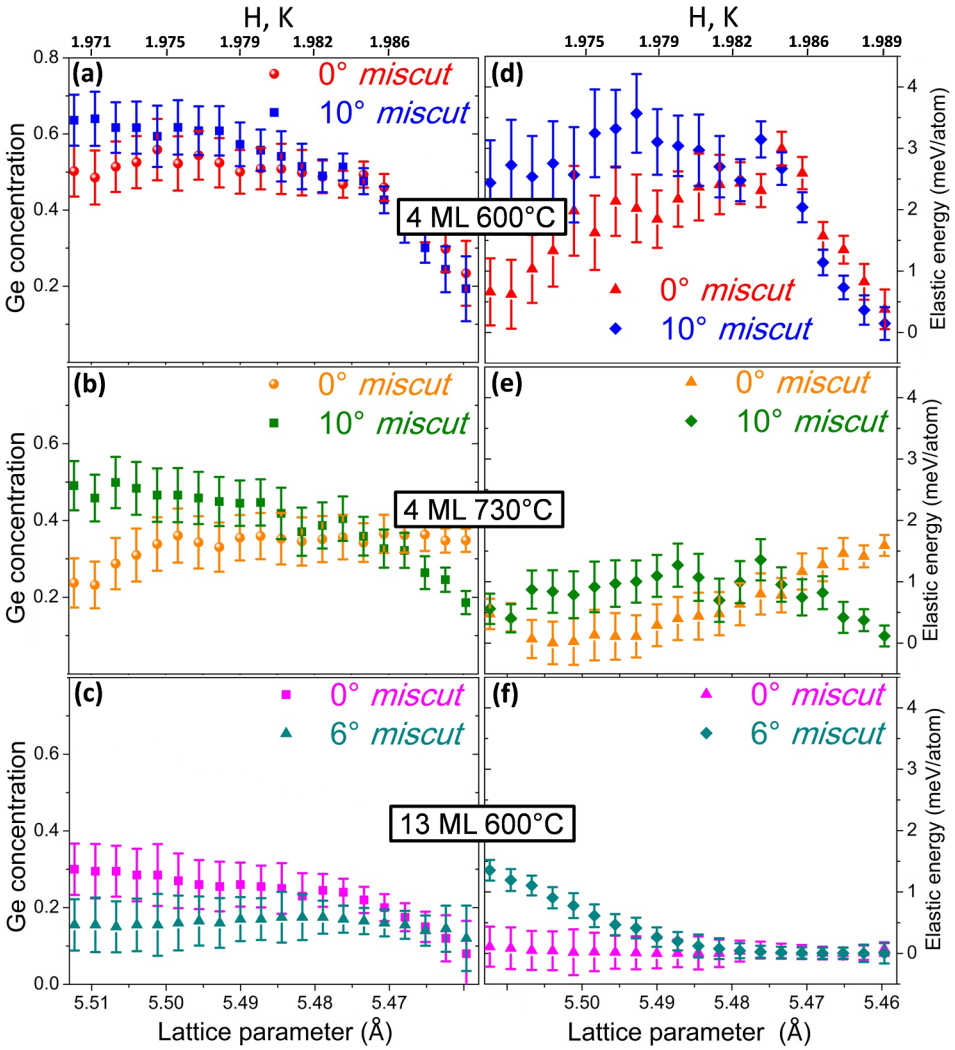

Fig. 5. Ge concentrations for samples grown at (a) 600 °C (4 ML Ge), (b) at 730 °C (4 ML Ge) and (c) at 600 °C (13 ML Ge), with 0° and 10° miscut for the first two sets of samples and 0° and 6° miscut for the set of panel (c). The elastic energy per atom (in meV/atom) is shown for the samples (d) 600 °C (4 ML Ge), (e) 730 °C (4 ML Ge) and (f) 600 °C (13 ML Ge). Higher energies values are generally observed for the samples grown at substrates with miscut.

FEM (bulk-like) simulations. For instance, the second principal strain (that depends on the difference of the in-plane directional strains) along a vertical line drawn in the geometrical center of the domes is different for the two geometries. The second principal strain is defined as: $\varepsilon_{II} = \frac{\varepsilon_x + \varepsilon_y}{2} - \frac{1}{2}\sqrt{(\varepsilon_x - \varepsilon_y)^2 + Y_{xy}^2}$, where $\varepsilon_i = \frac{\partial u_i}{\partial i}$ is the derivative of the displacement along the i direction with respect to the same direction and $Y_{xy} = \frac{\partial u_y}{\partial x} + \frac{\partial u_x}{\partial y}$ is the shear strain component. The profiles extracted from our simulations are depicted in Fig. 6(b) for both structures along the growth direction (out-of-plane), with and without miscut. The plot again points out a strong strain asymmetry in the 10° miscut sample.

Longitudinal x-ray diffraction scans on samples with 0° and 10° miscut, shown in Fig. 7(a), show an additional broadening of the diffraction peak of Ge islands in case of non-zero miscut. To check whether the asymmetry observed by FEM simulations in the bulk of the islands is related to the broadening of the island diffraction peak, we simulated the x-ray diffraction radial scans from the FEM structures. The result is shown in Fig. 7(b). The theoretical curves do not exhibit a significant difference for low (H, K) values, indicating that the effect observed in the experiment may not come from the bulk elastic energy, but from the miscut-induced facets, which introduce strain states that cannot be retrieved in the flat substrate systems.

Another series of FEM simulations on iso-volume islands were also analysed comparing domes with pure Ge content and with a $Si_{0.5}Ge_{0.5}$ alloy ratio. We retrieved the average elastic energy (in meV/atom) for three-dimensional islands simulated with a miscut of 0, 2°, 6° and 10°. The results are shown in Fig. 8 (dotted lines / solid dots), and are compared with those obtained experimentally, displayed as dashed lines/open dots. The size of the marks takes into account the error bar on the vertical axis, while the energy scale (Y-axis) is logarithmic. The comparison has been done for the samples with 4 ML Ge coverage, grown at 600 °C (blue) and 730 °C (red), which are close in composition to simulated islands with pure Ge (dark blue) and a $Si_{0.5}Ge_{0.5}$ alloy structures (dark red).

The simulated pure Ge islands obviously exhibit the largest volume-averaged elastic energy (of about 5.5 meV/atom) [26,27]. This value iis not affected by the morphological asymmetry imposed by the island shape within the simulated miscut range. The experimental data for the islands grown at 600 °C clearly show a lower average strain energy density with respect to the simulations with pure Ge content. This indicates a significant intermixing on both the flat and the misoriented substrates. What is indeed remarkable, in the experiment at 600 °C, is that the volume averaged strain energy increases strongly for the 10° miscut domes, going from an approximately 1.4 meV/atom value for islands grown on flat surfaces to 2.9 meV/atom on the miscut substrate. Since FEM simulations indicate that this asymmetry is not a bulk effect, we believe that the appearance of miscut-induced facets has indeed a crucial role in the storing of elastic energy in the real

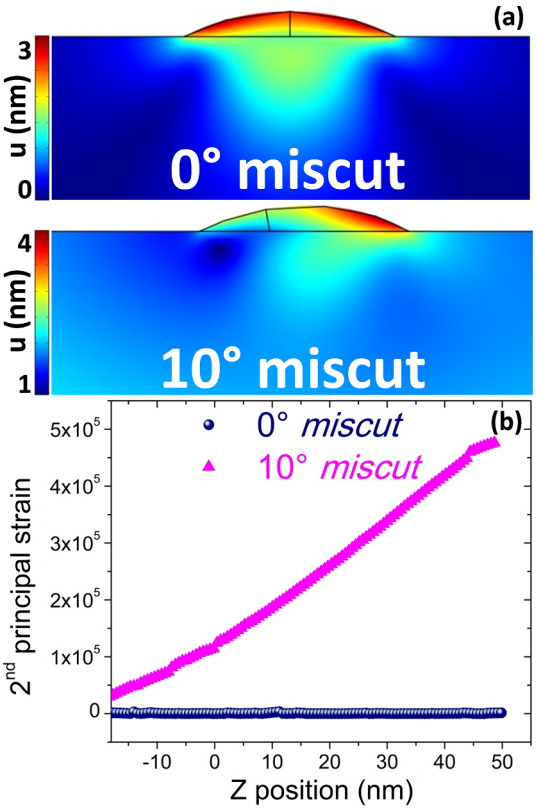

Fig. 6. (a) Cross-section maps for the structures simulated using a Finite Elements Method Simulation commercial software (COMSOL Multiphysics), representing islands with the experimental dimensions of domes with 4 ML Ge coverage grown at 600 °C for flat (upper panel) and 10° miscut (bottom panel) substrates. The colormap shows the total displacement ***u*** (sum of in-plane and out-of-plane) after relaxation, evidencing a strain asymmetry on the samples with miscut. Panel (b) shows the second principal strain corresponding for the structures depicted on figure (a) for the elements following a vertical (growth direction) line that passes through the geometrical center of the domes, endorsing the strain asymmetry present on the 10° miscut sample.

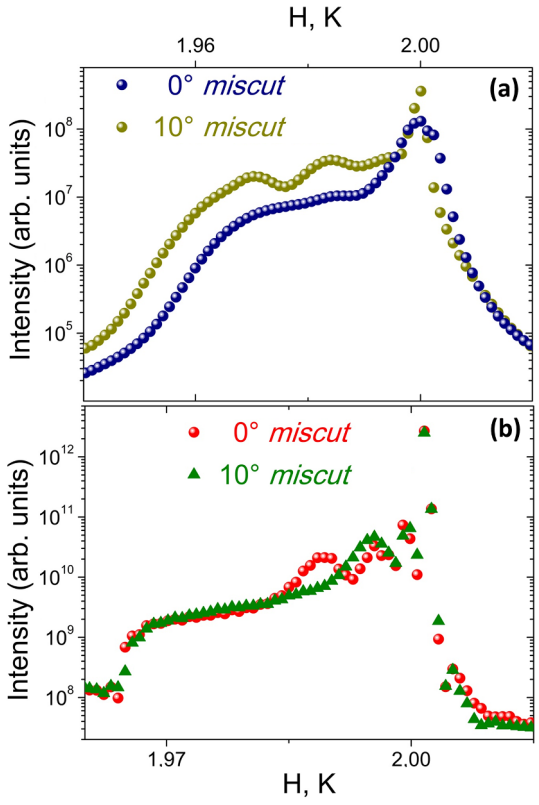

Fig. 7. (a) Experimental data for 0° and 10° miscut samples with 13 ML Ge coverage. (b) Simulated longitudinal x-ray diffraction scans, which indicate that the enlargement of the broad peak observed in the experimental curves [panel (a)] does not arise from the bulk elastic energy configuration.

(experimentally evaluated) system.

As expected, lower elastic energies are retrieved for the simulated islands with 50% Si content (about 1.1 meV/atom in Fig. 8), where again the miscut has no influence on the averaged energy if only bulk conditions are considered. These simulations can be compared to the volume-averaged anergies for the 730 °C samples, where intermixing is more severe. Again, for the 4 ML domes grown at substrates with miscut, we measure a larger average elastic energy with respect to their counterparts grown on the flat substrate. Experimentally, we evaluate a strain energy of 0.22 meV/atom for the 0° miscut substrate, while 0.85 meV/atom for the 10° miscut sample. Again, we believe that the difference in elastic energy is stored at the asymmetric facets for the samples with 10° miscut.

The observed difference of elastic energy among islands on distinct substrates (vicinal and with miscut) are quite high if compared in their average values. Namely, the effect of an asymmetric faceting at large miscuts on the energetic balance is comparable to a change in stoichiometry of about 20–30% in Si content. We speculate that both surface (kinetic) and bulk diffusion behave differently in assymetric domes. Surface diffusion may be affected by the distinct facet slope and surface reconstruction on the miscut domes, while bulk diffusion may be different for the islands shaped by the miscut due to the different height of the exposed surface (where the perpendicular stress is zero) with respect to the substrate/island interface, compared to the symmetric island shape on the flat substrate.

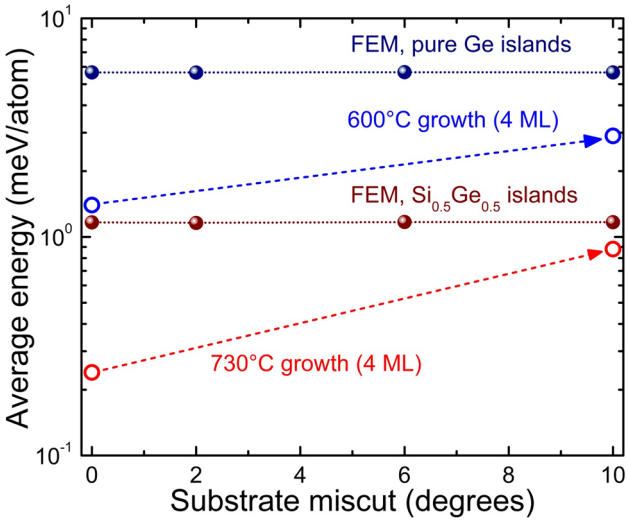

Fig. 8. Volume averaged energy (in meV/atom) for the structures simulated through FEM (dotted lines/solid dots) and obtained experimentally (dashed lines/open dots). Experimental results from samples with 4 ML Ge coverage grown at 600 °C (blue) and 730 °C (red) were compared with simulations assuming pure Ge islands (dark blue) and $Si_{0.5}Ge_{0.5}$ islands (dark red). The results point out to a larger elastic energy stored at the asymmetric facets for the samples with 10° miscut. Arrows connecting the experimental data serve as guide to the eyes only.

4. Conclusions

In conclusion, we have studied the intermixing inside SiGe islands grown on Si(0 0 1) substrates with and without miscut angle. Radial

anomalous x-ray diffraction measurements were performed on samples containing 4 ML and 13 ML of Ge, grown under 600 °C and 730 °C. The Ge concentration and the elastic energy per atom stored during the nanostructures formation process, were retrieved. Previous studies on the flat Si(0 0 1) surface have shown that the Ge domes evolve into superdomes and during this transition process relax [28–32], but as far as we know this is the first time that the Ge concentration and the stored elastic energy is quantified for these structures. A comparison between FEM analysis of the structures, suited for bulk-like behavior, and the experimental data indicates that the different values obtained for the elastic energy probably arise due to a non trivial effect of the miscut-induced facets on substrates with large misorientation angles. Islands grown on large miscut substrates present higher values of volume-averaged elastic energy. A distinct local Si intermixing at the asymmetric islands may be responsible for such effect. Therefore, besides modifications on island morphology and density, the introduction of non-flat substrates allows to tune the elastic energy stored inside the Ge islands.

Acknowledgements

The authors acknowledge FAPEMIG, CAPES, and CNPq for financial support. L.P. acknowledge the European Union's Horizon 2020 research and innovation programme under grant agreement No. 766719- FLASH project. Beamtime was granted on the ID01 and BM02 beamlines by the ESRF, as well as on the XRD2 and the XDS beamlines by the LNLS/MCTI.

References

[1] M. Schmidbauer, Sh. Seydmohamadi, D. Grigoriev, Zh.M. Wang, Yu.I. Mazur, P. Schäfer, M. Hanke, R. Köhler, G.J. Salamo, Controlling planar and vertical ordering in three-dimensional (In, Ga)As quantum dot lattices by GaAs surface orientation, Phys. Rev. Lett. 96 (2006) 066108–066108-4.
[2] O.G. Schmidt, N.Y. Jin-Phillipp, C. Lange, U. Denker, K. Eberl, R. Schreiner, H. Gräbeldinger, H. Schweizer, Long-range ordered lines of self-assembled Ge islands on a flat Si (001) surface, Appl. Phys. Lett. 77 (2000) 4139–4141.
[3] G. Costantinia, A. Rastelli, C. Manzano, R. Songmuang, O.G. Schmidt, K. Kern, Universal shapes of self-organized semiconductor quantum dots: striking similarities between InAs/GaAs(001) and Ge/Si(001), Appl. Phys. Lett. 85 (2004) 5673–5675.
[4] L. Persichetti, A. Sgarlata, M. Fanfoni, A. Balzarotti, Ripple-to-dome transition: the growth evolution of Ge on vicinal Si(1 1 10) surface, Phys. Rev. B 82 (2010) 121309–121309-4.
[5] L. Fazi, C. Hogan, L. Persichetti, C. Goletti, M. Palummo, A. Sgarlata, A. Balzarotti, Intermixing and buried interfacial structure in strained Ge/Si(105) facets, Phys. Rev. B 88 (2013) 195312–195312-6.
[6] L. Persichetti, A. Sgarlata, G. Mattoni, M. Fanfoni, A. Balzarotti, Orientational phase diagram of the epitaxially strained Si(001): evidence of a singular (105) face, Phys. Rev. B 85 (2012) 195314–195314-6.
[7] L. Persichetti, A. Sgarlata, M. Fanfoni, A. Balzarotti, Shaping Ge islands on Si(001) surfaces with misorientation angle, Phys. Rev. Lett. 104 (2010) 036104–036104-4.
[8] A. Sgarlata, L. Persichetti, A. Capasso, M. Fanfoni, N. Motta, A. Balzarotti, Driving Ge island ordering on nanostructured Si surfaces, Nanosci. Nanotechnol. Lett. 3 (6) (2011) 841–849.
[9] L. Persichetti, A. Sgarlata, M. Fanfoni, A. Balzarotti, Heteroepitaxy of Ge on singular and vicinal Si surfaces: elastic field symmetry and nanostructure growth, J. Phys.: Condens. Matter 27 (2015) 253001–1-28.
[10] L. Persichetti, A. Sgarlata, M. Fanfoni, A. Balzarotti, Pair interaction between Ge islands on vicinal Si(001) surfaces, Phys. Rev. B 81 (2010) 113409–113409-4.
[11] B. Yang, F. Liu, M.G. Lagally, Local strain-mediated chemical potential control of quantum dot self-organization in heteroepitaxy, Phys. Rev. Lett. 92 (2004) 025502–025502-4.
[12] L.A.B. Marçal, B.L.T. Rosa, G.A.M. Safar, R.O. Freitas, O.G. Schmidt, P.S.S. Guimarães, Ch. Deneke, A. Malachias, Observation of emission enhancement caused by symmetric carrier depletion in III-V nanomembrane heterostructures, ACS Photonics 1 (2014) 863–870.
[13] L. Persichetti, R. Menditto, A. Sgarlata, M. Fanfoni, A. Balzarotti, Hug-like island growth of Ge on strained vicinal Si(111) surfaces, Appl. Phys. Lett. 99 (2011) 161907–161907-3.
[14] J. Tersoff, C. Teichert, M.G. Lagally, Self-organization in growth of quantum dot superlattices, Phys. Rev. Lett. 76 (1996) 1675–1678.
[15] J. Stangl, V. Holý, G. Bauer, Structural properties of self-organized semiconductor nanostructures, Rev. Mod. Phys. 76 (2004) 725–783.
[16] B. Voigtländer, Fundamental processes in Si/Si and Ge/Si epitaxy studied by scanning tunneling microscopy during growth, Surf. Sci. Rep. 43 (43) (2001) 127–254.
[17] I. Berbezier, A. Ronda, SiGe nanostructures, Surf. Sci. Rep. 64 (2009) 47–98.
[18] A. Vailionis, B. Cho, G. Glass, P. Desjardins, David G. Cahill, J.E. Greene, Pathway for the strain-driven two-dimensional to three-dimensional transition during growth of Ge on Si(001), Phys. Rev. Lett. 85 (2000) 3672–3675.
[19] A. Rastelli, H. Von Känel, B.J. Spencer, J. Tersoff, Prepyramid-to-pyramid transition of SiGe islands on Si(001), Phys. Rev. B 68 (2003) 115301–115301-6.
[20] J. Tersoff, B.J. Spencer, A. Rastelli, H. von Känel, Barrierless formation and faceting of SiGe islands on Si(001), Phys. Rev. Lett. 89 (2002) 196104–196104-4.
[21] L. Persichetti, A. Sgarlata, M. Fanfoni, A. Balzarotti, Breaking elastic field symmetry with substrate vicinality, Phys. Rev. Lett. 106 (2011) 055503–055503-4.
[22] A. Malachias, M. Stoffel, M. Schmidbauer, T. Schulli, G. Medeiros-Ribeiro, O.G. Schmidt, R. Magalhaes-Paniago, T.H. Metzger, Atomic ordering dependence on growth method in Ge:Si(001) islands: influence of surface kinetic and thermodynamic interdiffusion mechanisms, Phys. Rev. B 82 (2010) 035307–035307-9.
[23] L.A.B. Marçal, M.S.C. Mazzoni, L.N. Coelho, E. Marega, G.J. Salamo, R. Magalhães-Paniago, A. Malachias, Quantitative measurement of manganese incorporation into (In, Mn)As islands by resonant x-ray scattering, Phys. Rev. B 96 (2017) 245301–245301-7.
[24] A. Marzegalli, V.A. Zinovyev, F. Montalenti, A. Rastelli, M. Stoffel, T. Merdzhanova, O.G. Schmidt, Leo Miglio, Critical shape and size for dislocation nucleation in $Si_{1-x}Ge_x$ islands on Si(001), Phys. Rev. Lett. 99 (2007) 235505–235505-4.
[25] F. Montalenti, D. Scopece, L. Miglio, One-dimensional Ge nanostructures on Si(001) and Si(1 1 10): dominant role of surface energy, Comptes Rendus Phys. 14 (7) (2013) 542–552.
[26] R. Magalhaes-Paniago, G. Medeiros-Ribeiro, A. Malachias, S. Kycia, T.I. Kamins, R. Stan Williams, Direct evaluation of composition profile, strain relaxation, and elastic energy of Ge:Si(001) self-assembled islands by anomalous x-ray scattering, Phys. Rev. B 66 (2002) 245312–245312-6.
[27] G. Medeiros-Ribeiro, A. Malachias, S. Kycia, R. Magalhães-Paniago, T.I. Kamins, R. Stanley Williams, Elastic energy mapping of epitaxial nanocrystals, Appl. Phys. A 80 (2005) 1211–1214.
[28] T.I. Kamins, G.M. Ribeiro, D.A.A. Ohlberg, R.S. Williams, Evolution of Ge islands on Si(001) during annealing, J. Appl. Phys. 85 (1999) 1159–1171.
[29] A. Rastelli, H. von Känel, Surface evolution of faceted islands, Surf. Sci. 515 (2002) L493–L498.
[30] T. Merdzhanova, S. Kiravittaya, A. Rastelli, M. Stoffel, U. Denker, O.G. Schmidt, Dendrochronology of strain-relaxed islands, Phys. Rev. Lett. 96 (2006) 226103–226103-4.
[31] M.I. Richard, T.U. Schülli, G. Renaud, E. Wintersberger, G. Chen, G. Bauer, V. Holý, In situ x-ray scattering study on the evolution of Ge island morphology and relaxation for low growth rate: advanced transition to superdomes, Phys. Rev. B 80 (2009) 045313–045313-9.
[32] M.I. Richard, G. Chen, T.U. Schülli, G. Renaud, G. Bauer, Coalescence of domes and superdomes at a low growth rate or during annealing: towards the formation of flat-top superdomes, Surf. Sci. 602 (2008) 2157–2161.